https://doi.org/10.52326/ic-ecco.2021/TAP.02

Solution-processed bulk heterojunction solar cells based on a zinc phthalocyanine: perylene dimiide derivative

V. Furtuna[1], I. Lungu[2], I. Gadiac[3] and T. Potlog[4]
[1,2,3,4] Moldova State University, A. Mateevici 60, MD 2009, Chisinau Moldova
e-mail: tpotlog@gmail.com, www.usm.md

***Abstract*—A solution processed ZnPc:PTDCI bulk heterojunction solar cells doped with iodine were fabricated and characterized. Photovoltaic properties of the solar cells were investigated by optical absorption, current density-voltage characteristic and external quantum efficiency. The absorption of ZnPc:I_2:PTDCI was observed in the (300-800) nm region. Solar cells with a power conversion efficiency of about 2.4% has been obtained using simply drop casting and spin-coating methods without special treatment. The peak of the external quantum efficiency characteristics of the ITO/PEDOT:PSS/ZnPc:I_2:PTCDI/Al solar cells is 10%.**

***Keywords*—zinc phthalocyanine; iodine; N,N′-Bis(3-pentyl)perylene-3,4,9,10-bis(dicarboximide); solar cell**

I. INTRODUCTION

Organic solar cells based on bulk heterojunctions (BHJ) from solution are attracting more and more attention due to the potential for mass production on a flexible and lightweight substrate. In the recent years, significant improvements have been made in BHJ solar cells by combining the molecular design of active materials and interface layers, morphology control, manufacturing techniques. The power conversion efficiencies over 9% have been achieved.

Zinc(II) phthalocyanine (ZnPc) have been frequently used as a photo-active layer in photovoltaic applications. Most of these applications are related to structure of dye-sensitized solar cells (DSSC) [1-4]. These compounds have also been used as a donor in bilayer photovoltaic devices [5]. Many researchers have been attended to conductive polymer based organic solar cells due to their easily and cheaply production [6]. Researchers have concentrated their work on hybrid-structured (organic-inorganic, organic-MPcs, organic-inorganic nanoparticles or quantum dots) solar cells as a solution to enhance the power conversion efficiency of organic solar cells [7,8]. ZnPc is generally used in DSSC based solar cells owing to higher power conversion efficiency due to their high optical absorption in the visible region [9]. Moreover, perovskite solar cells (PSCs) devices produced using phthalocyanine compounds have achieved excellent power conversion efficiencies. Higher PCEs values were obtained for unsymmetrically ZnPc compounds containing different substituents such as carboxyl and three tert-butyl groups [10,11] and symmetrically ZnPc compounds bearing four tertbutyl [12] or tetra-methoxyltriphenylamine groups [13,14]. The perovskite solar cells containing ZnPc with one carboxyl and three tert-butyl groups show (16 ± 1) mA/cm^2 photocurrent and (0.95 ± 0.07) V open circuit voltage resulting in (13.0 ± 0.7)% PCE at 1 sun [15]. On the other hand, the dimeric Pcs are also used for this purpose with 14.4% PCEs values [16]. The solar cells based on a blend of ZnPc and Buckminster fullerene C60 reached value of PCE as high as 1.9% for single *p-i-n* structures [17].

The disadvantage of solar cells based on bulk heterojunction based on phthalocyanines-fullerenes is that fullerenes are essential as an electron-acceptor material, but they absorb poorly visible light, reducing the volume of the fraction occupied by the donor material with high absorption power. Moreover, fullerenes have a low tunneling capacity, leading to restrictions placed on the development of conjugate systems for many attractive electronic structures to create higher short circuit current density. In this paper we will replace these fullerenes with perylene dimiides (PTCDIs) derivatives that would contribute to better electronic tunneling of carries [18]. These substances also ensure good mobility of the carriers, are processable in solutions and have a good light absorption in the visible spectrum, a high fluorescence quantum yield, and high electron affinity. For these reasons they are very promising candidates for application in organic solar cells [19]. Due to these properties, the representatives of the given family of organic substances are potential competitors of fullerenes in the production of photovoltaic devices. PTCDIs are one class of the most explored organic fluorescent materials due to their high luminescence efficiency, optoelectronic properties, and ready to form well-tailored supramolecular structure.

In this study we use a PTCDI derivative that acts as an electron acceptor organic material, while ZnPc corresponds to a donor to form bulk heterojunctions from

https://doi.org/10.52326/ic-ecco.2021/TAP.02

chemical solution. From the available literature and to the knowledge of the authors the investigations have not been carried out on the solution processable zinc phthalocyanine-PTCDI bulk heterojunction thin films solar cells. In this paper, we are reporting the structural, optical properties of ZnPc-PTCDI blend and photovoltaic parameters of the Organic Solar Cells (OPV) based on ZnPc-PTCDI thin films bulk heterojunctions.

II. SYNTHESIS OF ZNPC:PTCDI THIN FILMS AND DEVICES

Commercially available zinc phthalocyanine and N,N′-Bis(3-pentyl)perylene-3,4,9,10-bis(dicarboximide) (PTCDI) powders (98% purity) were purchased from Sigma Aldrich and were used without further purification. The formic acid (FA) (99% purity) also, purchased from Sigma Aldrich were selected as the solvent for ZnPc and PTCDI. The ZnPc powder was added to the solvent of 98% concentrations of formic acid (FA). In the ZnPc/FA solution the aggregation of undissolved ZnPc was observed. The solution was prepared by dissolving the ZnPc at a concentration of 1 mg/ml into FA solvent. The same procedure for solubilization of the N, N'-bis (3-pentyl) perylen-3,4,9,10-bis (dicarboximide) was used: 1.0 mg/ml in FA. To improve the conductivity of ZnPc and PTCDI thin films, they were doped with iodine. Both ZnPc and PTCDI solutions were sonicated for 1 hour and then were mixed in the different weight ratios. The structure of the films was analyzed by X-ray Bruker D8 advanced diffractometer (using CuK_α radiation with λ=1.5406 Å). The crystallite size (D) was calculated from the XRD patterns according to the well-known Scherer equation [20]:

$$D = \frac{0.9\,\lambda}{\beta \cos\theta}, \qquad (1)$$

where β is the full-width at half-maximum (FWHM) peak for a Bragg angle θ, and λ is the wavelength of the X-ray radiation. The structure was also investigated with Raman spectroscopy at an excitation light wavelength of 532 nm. The optical absorption spectroscopy of the ZnPc:I_2:PTCDI blend films at different composition was measured using a JASCO 7600 UV–Vis-NIR spectrophotometer. For the device fabrication the ZnPc:I_2:PTCDI on ITO glass substrates (~8 Ω/□) were synthetized. To increase the work function of the ITO oxide and to improve the electrical connection between ITO and organic active layer, a layer of PEDOT:PSS was spin-coated. An Al electrode was thermally deposited onto the ZnPc:I_2:PTCDI layer using a vacuum deposition system at a pressure of about 5 x 10^{-4} Pa. The current density–voltage (J–V) characteristics were measured under 100 mW cm^{-2} solar simulator using a Keithley 2400 Source-Meter-Unit. External quantum efficiency (EQE) measurements were measured using 90 W Xenon lamp as light source connected *via* an optical fiber to an ACTON Spectra Pro150 monochromator and an EG&G 7260 DSP Lock-in amplifier. The key device photovoltaic parameters such as fill factor (FF) can be estimated by [21]:

$$FF = \frac{P_m}{J_{SC} V_{OC}} = \frac{J_m V_m}{J_{SC} V_{OC}} \qquad (2)$$

where P_m is the maximum power generated, with the current density and voltage marked as J_m and V_m, and J_{SC} is the shortcircuit current density, V_{OC} .open-circuit voltage. The shunt R_{sh} and serie R_s rezistances are the important factors that limit the FF of solar cells.

The power conversion efficiency (PCE) can be calculated by [21]:

$$\eta = \frac{P_m}{P_{in}} = \frac{J_m V_m}{P_{in}} = \frac{J_{SC} V_{OC} FF}{P_{in}} \qquad (3)$$

where P_{in} is the incident light power on the device.

III. STRUCTURAL AND OPTICAL PROPERTIES OF ZNPC:PTCDI THIN FILMS

The X-ray diffractograms of the undoped and ZnPc thin films doped with iodine (I_2) deposited from FA solution and thermally annealed at different temperatures are presented in Figure 1 .

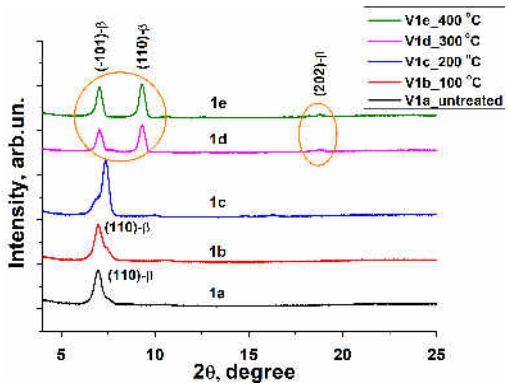

Figure 1. The XRD patterns of untreated and thermally annealed ZnPc:I_2 thin films at different temperatures: V1a- untreated, thermarly annealed : V1b – 100 °C, V1c- 200 °C, V1d- 300 °C, V1e- 400 °C.

According to the data revealed in the Figure 1, it can be stated that the transition from α-β phases to a single stable β phase occurs in the temperature range of 200-300°C. Zinc phthalocyanine powder (purchased from Sigma Aldrich used without further purification) from which all the thin films were synthesized, was present in the β crystalline phase [22]. It seems that the protic solvent FA has an essential impact on the ZnPc. Likewise, doping with iodine influences the ZnPc component. Also in this temperature range, as can be seen from the diffractograms shown in Figure 2 (a) for the ZnPc:I_2:PTCDI thin layers V3a, V3b, V3c, V3d and V3e, resulting from the disappearance of intense maxima at

https://doi.org/10.52326/ic-ecco.2021/TAP.02

2θ=5.26 degrees, that means complete elimination occurs of the PTCDI component from the thin layers. On the other hand, from the data presented in the XRD diffractograms from figure 2 (b) for thin layers V4a, V4b, V4c, V4d, V43, and from the comparative analysis of diffractograms for V3d and V4d samples, we revealed that iodine doping has a certain influence on the retention in the layers of PTCDI component even at temperatures above 300 °C. This suggests firstly the preservation of a certain amount of iodine (more likely the ionic type) in the analyzed systems, and secondly it indicates the intensification of interactions at the boundaries of the ZnPc and PTCDI phases.

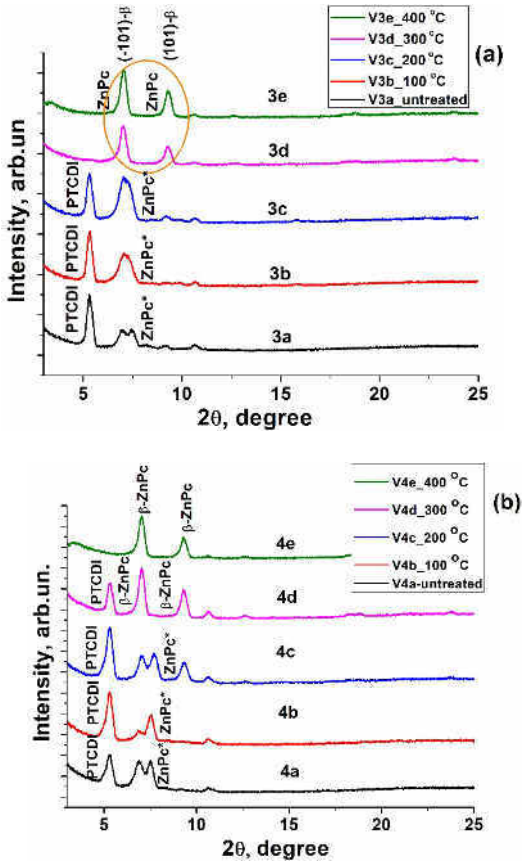

Figure 2 (a, b). The XRD patterns of untreated and thermally annealed ZnPc:I_2:PTCDI thin films at different temperatures, V3a, V4a - untreated, thermally treated V3b, V4b – 100 °C, V3c, V4c – 200 °C, V3d, V4d- 300 °C, V3e, V4 e- 400 °C.

It follows that the stabilization of the β-phase of zinc phthalocyanine thin films during annealing and the simultaneous preservation of certain iodine species and the PTCDI perylene acceptor component due to the intensification of ZnPc and PTCDI interactions, should contribute to the facilitation of electrical charge transfer at the interface of these components in the volume of heterojunctions obtained on the basis of thin layers of the given type. To confirm the presence of iodine species in the doped thin layers, Raman analysis was performed. In Fig. 3 it has been found that all Raman signals for ZnPc after iodine doping decrease. The presence of $ZnI_2(HCOO)_2PcH_2$ molecular complex in Fig. 3 is revealed by the signal located at 164 cm^{-1}. Such a band has been observed in several publications [22-24]. In addition, iodine doping contributes to the broadening of the signal corresponding to the tensile vibrations of the isoindole units at 1335 cm^{-1} and to the disappearance of the signal corresponding to the tensile vibrations of the pyrrole unit at 1580 cm^{-1}.

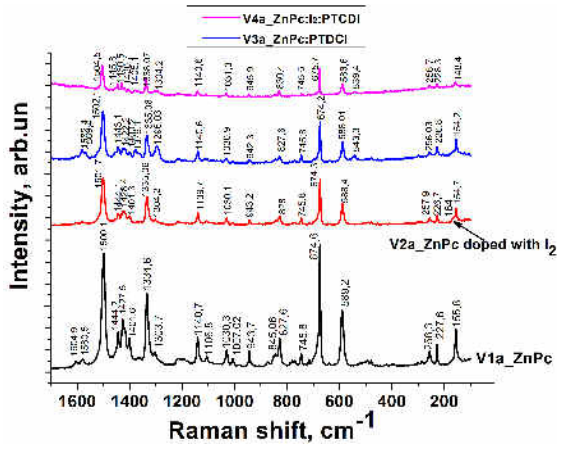

Figure 3. Raman spectra of undoped V1a, V3a ZnPc and ZnPc:PTCDI thin films and doped with iodine -V2a, V4a, respectively.

For the ZnPc thin layer doped with iodine and thermally annealed at 100°C for 30 minutes, the signal attenuation was recorded at 164 cm^{-1} (Figure 4), and for those anealed at higher temperatures, the disappearance of this signal was found. These findings suggest the removal of molecular iodine from the thin films, and the gradual desorption of iodide ions from the ZnIx(HCOO)yPcH2 complex during annealing.

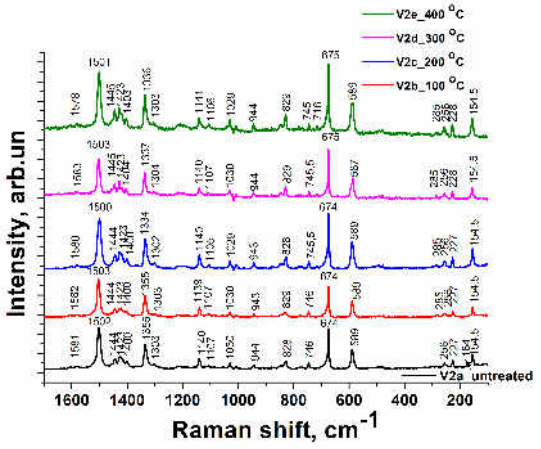

Figure 4. Raman spectra for untreated V2a and thermally annealed V2b, V2c, V2d and V2e ZnPc thin films obtained from doped 4ZnPc:1I_2/FA saturated solution.

https://doi.org/10.52326/ic-ecco.2021/TAP.02

The absorption spectra were measured for saturated solutions where molar concentration of ZnPc was 4.32 mol · m^{-3}. The absorption spectra are presented in Fig. 5. The absorption spectrum of ZnPc thin film obtained by thermal evaporation in vacuum, the two solvatochromic bands Q and B presents [25].

The Q band occurs due to the transition from the ground state a_{1u} (π) HOMO to e_g (π *) LUMO. The Q band splits into three distinct peaks. The splitting of the Q band is probably due to the vibration coupling in the excited state. [26]. The bands situated at 1.92 eV and 1.73 eV involve the transitions a_{1u} to e_g and $2a_{2u}$ to $7e_g$ in ZnPc macrocycle, and the one at 1.65 eV can be attributed to the excitonic transition or vibrational region. The appearance of the solvatochromic B Soret band with the two peaks located at 3.39 eV and 3.72 eV can be attributed to the π-π* transition [25]. The absorbance spectrum for the saturated ZnPc/FA solution shows the same absorption Q and B bands, but they are wider and shifted to longer wavelengths, compared to those of the ZnPc layer obtained by vacuum thermal evaporation [27]. Probably, the shift of the solvatochromic bands are due to the interactions of zinc phthalocyanine with the FA solvent, resulting in the formation of supramolecular Zn(HCOOH)xPc complexes.

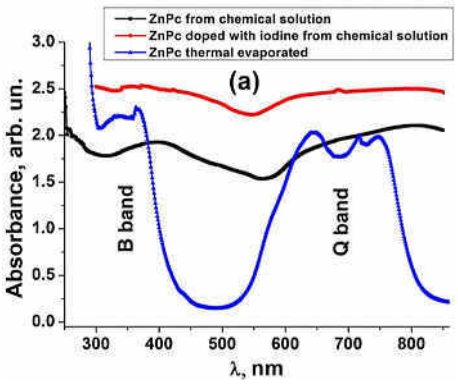

Figure 5. The absorption spectra for undoped and doped ZnPc thin films prepared from ZnPc/FA solutions and ZnPc thin film obtained by thermal vacuum evaporation.

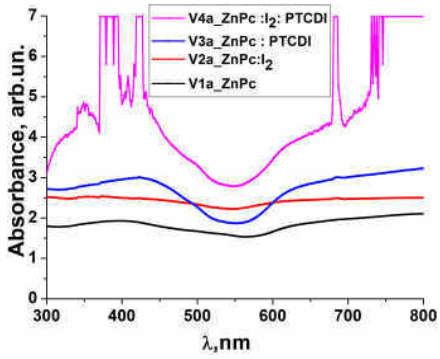

Figure 6. The absorption spectra for undoped ZnPc and ZnPc:PTCDI thin films and doped with iodine in formic acid.

The absorbance spectra of undoped ZnPc, ZnPc:PTCDI (ratio proportion (2:1)) and doped with iodine in formic acid are illustrated in Figure 6. It is observed that the absorption spectrum of ZnPc:I_2:PTCDI is more structured than that of the undoped mixture. At the same time, we find that iodine doping contributes to the increase of the absorbance intensity and the spectrum shows more intense peaks in both Q and B solvatochromic bands. According to the reference [23], at a sufficiently high ratio of I: Zn in aqueous solutions it is possible to form complexes with changing Zn^{2+} coordination from the octahedral configuration to the tetrahedral configuration. The presence of these well-pronounced peaks demonstrates the formation of the supramolecular complex due to the self-assembly of ZnPc:I_2 and PTCDI in saturated solutions.

IV. SOLAR CELLS CHARACTERIZATION

The ITO glass substrates with ~8 Ω/Square resistivity were sonicated in acetone, in ethanol and dried under hydrogen flow. Then a 120 nm thick buffer layer of PEDOT: PSS was spin-coated onto a ITO substrate at 2500 rpm and subsequently annealed in vacuum at 150°C for 30 min. The absorber layer of the bulk heterojunction solar cell is made of ZnPc:I_2 donor and PTCDI acceptor molecules.

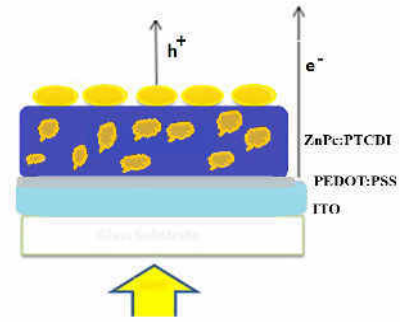

Figure 7. The schematic configuration of solution processable glass/ITO/ PEDOT:PSS/ZnPc:I_2:PTCDI/Al solar cell.

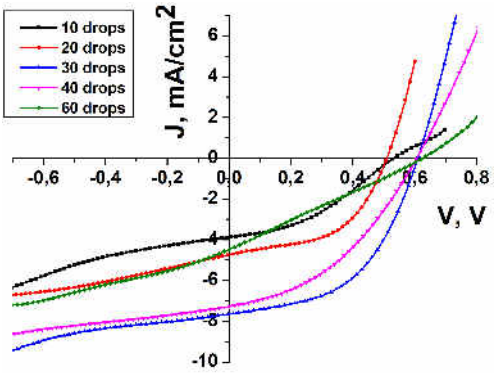

Figure 8. The current density–voltage (J–V) characteristics of ITO/PEDOT:PSS/ZnPc:I_2:PTCDI/Al solar cells.

https://doi.org/10.52326/ic-ecco.2021/TAP.02

A solution of ZnPc:I_2:PTCDI in 98% of FA was made and was dropped on the glass/ITO/PEDOT:PSS substrate. The solution-processable bulk heterojunctions solar cells consists of glass/ITO/PEDOT:PSS/ZnPc:I_2:PTCDI structure. Finally, aluminum (Al) electrodes were higher vacuum thermally evaporated. The incident light enters in the device through transparent ITO side and is absorbed in ZnPc:I_2:PTCDI. The absorbed photons result in the creation of bound electron-holes pairs in the absorbing layer, called excitons. Some of these excitons diffuse to the ZnPc:I_2:PTCDI/Al interface where dissociate to electrons and holes. The schematic configuration of solution processable glass/ITO/ PEDOT: PSS/ZnPc: I_2: :PTCDI/Al solar cell is shown in Figure 7.

The photovoltaic parameters are presented in Table 1.

TABLE I. The photovoltaic parameters: current-density (J_{sc}), open circuit voltage (Uoc), fill factor (FF) and efficiency (η), series (R_s) and shunt (R_{sh}), resistances of ITO/PEDOT:PSS/ZnPc: I_2: PTCDI/Al solar cells

drops	J_{SC}, mA/cm^2	U_{CD}, V	FF, %	η, %	R_S, Ohm·cm^2	R_{SH}, Ohm·cm^2
10	3.9	0.53	37.16	0.77	113.17	529.02
20	4.7	0.51	50.97	1.23	21.00	307.87
30	7.6	0.61	51.25	2.39	19.81	458.79
40	7.3	0.60	40.91	1.81	35.13	405.74
60	4.6	0.62	24.85	0.71	109.35	161.11

According to the Table 1 the photovoltaic parameters of ITO /PEDOT:PSS/ZnPc:I_2:PTCDI/Al depend on the layer thickness (solution volume). It is observed that initially, with the increase of the layer thickness (number of drops), the open circuit voltage decreases, and then it starts to increase. The density of the short-circuit current increases with the increase of the thickness (number of drops) and at the highest thickness it decreases and reaches the value of 4.6 mA /cm^2. This current-density corresponds to the highest value of the open circuit voltage of 0.62 V. It is well known that the behavior of the p–n junction is simulated by a diode, and the current losses (such as bulk resistances of materials and electrodes, or current leakage) can be modeled by series resistance (R_s) and shunt resistance (R_{sh}), respectively. It is widespread proved that the equivalent circuit model is applicable to organic solar cells. Therefore the shape of the J–V curves can be limited by the three elements in the equivalent circuit model. These are FF , R_s and R_{sh}. The FF is the parameter that determine the PCE of organic solar cells. R_s induces a voltage drop on itself, so it can divide the applied voltage from the diode. Therefore the larger the R_s is, the less voltage drop on the diode, which results in a slower increase of J with V. R_{sh} has the effect of dividing current from diode, which makes it exhibit the opposite trend to that of R_s. When a reverse bias is applied, J should be small for the blocking effect of diode under reverse bias. However if R_{sh} is small, then the current under reverse bias will flow into R_{sh} and J will increase linearly with the increasing reverse voltage. This will also lower FF. In the fabricated solar cells, reduction of R_s is effective means to improve the performance of the device. Also, the thickness of the blend layer, the interface between the active layer and electrodes, and the illumination intensity are three variables that can influence R_{sh} and ultimately impact on FF. The dominating contribution to the R_s is caused by the large resistivity of the ZnPc:I_2: :PTCDI organic thin films. The best efficiency of conversion of solar energy into electricity for ITO/ PEDOT:PSS/ZnPc:I_2: :PTCDI/Al solar cell reaches the value of about 2.4%.

The external quantum efficiency (EQE) for the ITO/ PEDOT:PSS/ZnPc:I_2:PTCDI/Al structure is illustrated in Figure 9. The study of the distribution of external quantum efficiency showed that the photosensitivity range is between 300 nm and 800 nm wavelengths. Photosensitivity of the ITO/ PEDOT:PSS/ZnPc:I_2: :PTCDI/Al structure is higher from 500 nm to 800 nm, and as the thickness of the ZnPc:I_2:PTCDI layer increases, the external quantum efficiency decreases.

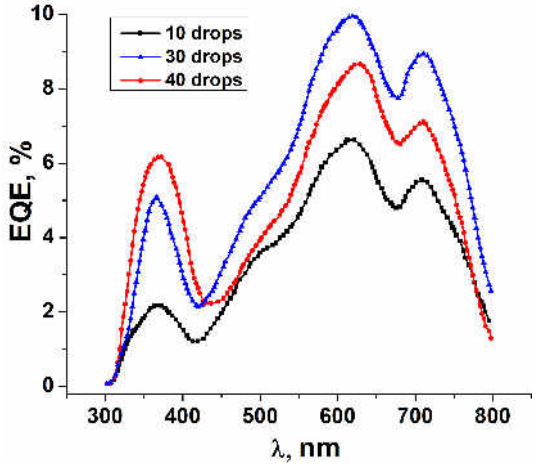

Figure 9. The external quantum efficiency characteristics of the ITO/ PEDOT:PSS/ZnPc:I_2:PTCDI/Al solar cells.

The charge transfer (CT) is affected by recombination during the move of electrons and holes to the electrodes, especially if are transported by the same material.

CONCLUSION

The solution-processable bulk heterojunctions solar cells with ITO/PEDOT:PSS/ZnPc:I_2:PTCDI structures using low cost drop casting and spin coating methods were fabricated. The optimized solar cell composition in this investigation is the 2:1:1 of the ZnPc:I_2:PTCDI mixture at which the J_{SC}, V_{OC}, FF, and η are 7.6 mA/cm^2, 0.61 V, 0.51, and 2.39 %, respectively. The R_s has a pronounced effect on the shape of J–V curve around V_{OC}, large R_s divide the voltage from the diode, leading to a slower rise of J with increasing positive V and FF decreases.

https://doi.org/10.52326/ic-ecco.2021/TAP.02

ACKNOWLEDGMENT

The authors thank the Ministry of Education, and Research of the Republic of Moldova for funding research grants 20.80009.5007.16.

REFERENCES

[1] M. Grätzel, "Perspectives for dye-sensitized nanocrystalline solar cells," *Prog. Photovoltaic Res. Applic. Vol.* 8, pp. 171 – 185, 2000.

[2] Y. Reddy, L. Giribabu, C. Lyness, H. Snaith, C. Vijaykumar, M. Chandrasekharam, M. Lakshmikantam, J. Yum, K. Kalyanasundaram, M. Grätzel, M. Nazeeruddin, *Angew. Chem. Vol.* 119, pp. 377, 2007.

[3] L. Tejerina, M. V. Martínez-Díaz, M. K. Nazeeruddin, M. Grätzel, T. Torres, "Role of the Bulky Aryloxy Group at the Non-Peripheral Position of Phthalocyanines for Dye Sensitized Solar Cells," *ChemPlusChem. Vol*. 82, pp. 132-135, 2016.

[4] A. C. Yüzer, G. Kurtay, T. Ince, S. Yurtdaş, E. Harputlu, K. Ocakoglu, M. Güllü, C. Tozlu, M. Ince, "Solution-processed small-molecule organic solar cells based on non-aggregated zinc phthalocyanine derivatives: A comparative experimental and theoretical study," *Materials Science in Semiconductor Processing*, *Vol.* 129, pp. 105777, 2021.

[5] M. O. Zouaghi, Y. Arfaoui, B. Champagne, "Density functional theory investigation of the electronic and optical properties of metallo-phthalocyanine derivatives," *Optical Materials, Vol.* 120, pp. 111315, 2021.

[6] S. Günes, H. Neugebauer, and N. S. Sariciftci, "Conjugated Polymer-Based Organic Solar Cells," *Chem. Rev. Vol.* 107, pp. 1324–1338, 2007.

[7] C. Lungenschmied, G. Dennler, H. Neugebauer, S. Sariciftci, M. Glatthaar, T. Meyer, and A. Meyer, "Flexible, long-lived, large-area, organic solar cells," *Solar Energy Materials and Solar Cells Vol.* 91, pp. 379–384, 2007.

[8] M. Wright, A. Uddin, "Organic-inorganic hybrid solar cells: A comparative review," *Solar Energy Materials & Solar Cells. Vol.* 107, pp. 87–11189, 2012.

[9] J.-J. Cid, M. García-Iglesias, J.-H. Yum, A. Forneli, J. Albero, E. Martínez-Ferrero, … T. Torres, "Structure-Function Relationships in Unsymmetrical Zinc Phthalocyanines for Dye-Sensitized Solar Cells," *Chemistry - A European Journal, Vol.* 15(20), pp. 5130–5137, 2009.

[10] R. Milan, G.S. Selopal, M. Cavazzini, et al., "Dye-sensitized solar cells based on a push-pull zinc phthalocyanine bearing diphenylamine donor groups: computational predictions face experimental reality," *Sci Rep Vol.* 7, pp. 15675, 2017.

[11] G. Pozzi, et al., "Fluorous molecules for dye-senzitized solar cells: synthesis and photoelectrochemistry of unsymmetrical zinc phthalocyanine sensitizers with bulky fluorophilic donor groups," *J. Phys. Chem. C Vol*. 115, pp. 3777–3788, 2011.

[12] E. Dube, D. Oluwole, E. Prinsloo, and T. Nyokong, "A Gold–Chitosan Composite with Low Symmetry Zinc Phthalocyanine for Enhanced Singlet Oxygen Generation and Improved Photodynamic Therapy Activity," *New J. Chem*. *Vol.* 42 (12), pp. 10214–10225, 2018.

[13] Z. Cui, et al., "Soluble tetra-methoxyltriphenylamine substituted zinc phthalocyanine as dopant-free hole transporting materials for perovskite solar cells," *Organic Electronics, Vol.* 69, pp. 248–254, 2019.

[14] Z.H. Bakr, Q. Wali, A. Fakharuddin, L. Schmidt-Mende, T.M. Brown, R. Jose, "Advances in hole transport materials engineering for stable and efficient perovskite solar cells," *Nanomater. Energy Vol.* 34, pp. 271–305, 2017.

[15] E. Nouri, J.V. Krishna, C.V. Kumar, V. Dracopoulos, L. Giribabu, M.R. Mohammadi, P. Lianos, "Soluble tetratriphenylamine Zn phthalocyanine as hole transporting material for perovskite solar cells," *Electrochim. Acta Vol.* 222, 875–880, 2016.

[16] Y. Matsuo et. al., "Recent progress in porphyrin- and phthalocyanine-containing perovskite solar cells," *RSC Adv., Vol.* 10, pp. 32678-32689, 2020.

[17] M. Egginger, R. Koeppe, F. Meghdadi, P.A. Troshin, R.N. Lyubovskaya, D. Meissner, and N.S. Sariciftci, "Comparative studies on solar cell structures using zinc phthalocyanine and fullerenes," *Proc. SPIE 6192, Organic Optoelectronics and Photonics II*, pp. 61921Y, 26 April 2006.

[18] N. Enrique F. Sanchis, S. Seetharaman, P.A. Karr, Á. Sastre-Santos, F. D'Souza, F.F. Lázaro, "Directly Linked Zinc Phthalocyanine–Perylenediimide Dyads and a Triad for Ultrafast Charge Separation," Chemistry – *A European Journal Vol*. 25 (43), pp. 10123-10132, 2019.

[19] A. El-Refaey, S.Y. Shaban, M. El-Kemary, M. E. El-Khouly, "A light harvesting perylene derivative – zinc phthalocyanine complex in water: spectroscopic and thermodynamic studies," *Photochemical & Photobiological Sciences Vol.* 16(6), pp. 861-869, 2017.

[20] A. Valerio, Morelhao, et.al., "Usage of Scherrer's formula in X-ray diffraction analysis of size distribution in systems of monocrystalline nanoparticles," *MRS Advances* 2019.

[21] https://www.pveducation.org/pvcdrom/appendices/equati-xns/equations-for-photovoltaics.

[22] D.L. Hammick, M. Zvegintzov, "The Rate of Reaction Between Formic Acid And Iodine In Aqueous Solution," *J. Chem. Soc. Vol*. 129, pp. 1105–1108, 1926.

[23] Tammarugwattana, N., Mano, K., Watthanarungsarit, K., Rangkasikorn, A., Kayunkid, N., & Nukeaw, J. Study on Optical and Electrical Properties of Bismuth-Doped Nickel-Phthalocyanine Thin Films. Applied Mechanics and Materials, 848, 95–98, 2016. https://doi.org/10.4028/www.scientific.net/amm.848.95

[24] K.P. Madhuri, N. John, A. Subramanian, P. Santra, F.Bertram, "Influence of Iodine Doping on the Structure, Morphology and Physical Properties of Manganese Phthalocyanine Thin Films," *The Journal of Physical Chemistry C,* pp. 1-26*,* 2018.

[25] A.Farag, "Optical Absorption Studies of Copper Phthalocyanine Thin Films," *Opt. Laser Technol. Vol.* 39, pp. 728−732, 2007.

[26] K. Priya Madhuri, Pralay K. Santra, F. Bertram and Neena S. John, Influence of Iodine doping on the Structure and Properties of Metal-Phthalocyanine Thin Films
Phys. Chem. Chem. Phys., 2019, 21, 22955-22965;

[27] M. Wojdyła et al., "Absorption and photoreflectance spectroscopy of zinc phthalocyanine (ZnPc) thin films grown by thermal evaporation," *Materials Letters Vol.* 60, pp. 3441–3446, 2006.